INTERNATIONAL JOURNAL OF ENERGY RESEARCH
Int. J. Energy Res. (2011)
Published online in Wiley Online Library (wileyonlinelibrary.com). DOI: 10.1002/er.1937

Liquefied natural gas submerged combustion vaporization facilities: process integration with power conversion units

Giulio Tagliafico, Federico Valsuani and Luca A. Tagliafico*,†

Department of Engineering Production, ThermoEnergetics and Mathematical Models, Division of Thermal Engineering and Environmental Conditioning, DIPTEM/TEC, University of Genoa, Genoa, Italy

SUMMARY

Liquefied natural gas (LNG) vaporization facilities offer an excellent opportunity of primary energy saving by means of integration with power conversion units that is still weakly exploited in actual installations. This work focuses on the evaluation of primary energy saving achievable by the integration of an LNG vaporization facility with a gas turbine and with a cogenerative combined gas-steam power plant. The fuel energy saving ratio is used as the main performance parameter to evaluate the primary energy saving derived by system integration, with respect to conventional submerged combustion vaporization. Twelve possible configurations are analyzed with steady-state calculations. Results show that a primary energy saving greater than 15% with peak values up to 27%, corresponding to 2.98 TJ/year, is achievable. The paper shows that the fuel energy saving ratio can be used as a synthetic and effective parameter to estimate the energy-saving potential of different plant configurations. Copyright © 2011 John Wiley & Sons, Ltd.

KEY WORDS

liquefied; natural gas vaporization; cogeneration; fuel energy saving ratio

Correspondence

*Luca A. Tagliafico, DIPTEM/TEC, University of Genoa, Via all'Opera Pia 15/a, 16145, Genoa, Italy.
†E-mail: tgl@ditec.unige.it

Received 3 March 2010; Revised 14 July 2011; Accepted 8 August 2011

1. INTRODUCTION

Natural gas (NG) is a primary source of energy that covers the 20.5% of the world's total energy demand and the 22.6% of the Organization for Economic Cooperation and Development countries' total energy demand [1]. The NG must be conveyed in liquid state (liquefied NG (LNG)) with ship carriers, if the gas pipeline transportation is not economically convenient (i.e., large distances and sea crossing) or safe (crossing of independent countries). Vaporization facilities have a large amount of physical exergy stored in cryogenic tanks at −165 °C (the LNG in liquid state) that could be exploited in both direct (direct cooling) or indirect (plant integration) applications. Indirect applications are deepened in this paper, which presents a brief overview of the existing solutions and analyzes some plant configurations especially suited for the most commonly encountered LNG vaporization facilities.

In a vaporization facility, the LNG is discharged from LNG carriers and stored into cryogenic tanks, vaporized, and finally delivered, in a continuous process, to the NG main distribution network. The two main traditional vaporization technologies are the open rack vaporization (ORV) and the submerged combustion vaporization (SCV). The ORV uses a sea water mass flow rate to vaporize and warm up the LNG, whereas the SCV uses the combustion of a bleed of the main LNG stream. The ORV solution is eligible if the plant is close enough to a water source able to guarantee a very large water mass flow rate (for a 8 GSm^3/year vaporization facility, a mass flow rate as large as 30 000 m^3/h is required). The SCV solution is applied if there is no other thermal source available and the combustion of the NG itself is therefore needed to vaporize the LNG. For a 8 GSm^3/year vaporization facility, almost the 2% of the main LNG stream is burned by the SCV vaporization, with a great exergy and economic waste.

Figure 1 shows the scheme of a basic SCV vaporization facility. The LNG is stored in cryogenic tanks at −165 °C and 1.3 bar. Part of it (boil-off gas (BOG))

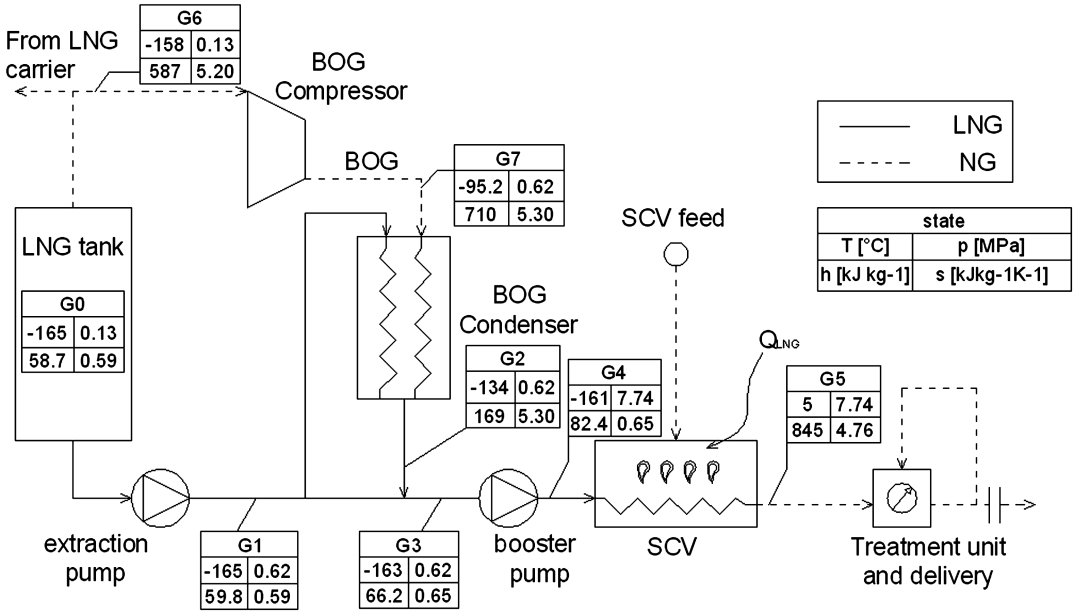

Figure 1. Scheme of the liquefied natural gas (LNG) vaporization process (submerged combustion vaporization (SCV) configuration). About 2% of the NG output is burned to vaporize the LNG main stream in the SCV (state G4), with great exergy losses. Typical operating data are reported in Table I.

boils because of thermal leakages in the tank. The BOG are condensed by a subcooled bleed of the main LNG stream and reintroduced into the main stream. The whole stream is pushed at high pressure (75 bar) through the SCV heat exchanger, and after a proper treatment (pressure, temperature, composition, Wobbe index, and water content requirements), the NG is delivered to the network. SCV burners are fed by another bleed of the main NG stream.

Figure 2 shows the thermodynamic transformations of the NG (assumed as pure methane) in the vaporization process. Typical values of the thermodynamic points G0,. . ., G7 are reported in Figure 1, whereas the process requirements are reported in Table I. The facility electrical requirements are usually met by a gas turbine (GT) with self-feeding purpose.

The first proposal of integration of LNG systems with power plants was developed by Greipentrog *et al*. [2,3], who, in 1976, analyzed a closed-loop gas cycle coupled to the LNG vaporization plant. Chiesa [4] analyzed four different plant configurations with the LNG vaporization process as a low temperature (−10 °C) heat sink. Desideri *et al*. [5] presented a solution with both heat recovery and LNG exploited as a cold thermal source. Hanawa proposed a closed-loop Ericsson cycle [6]. To maximize the efficiency in

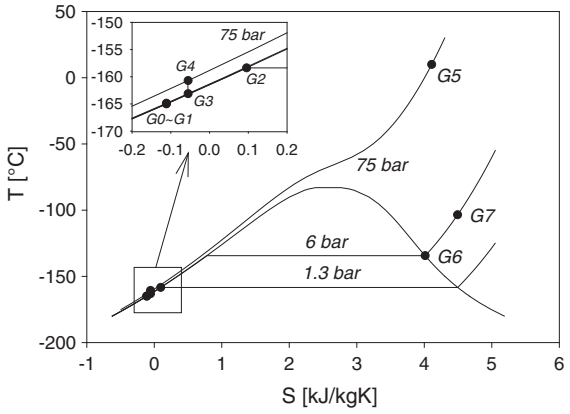

Figure 2. Thermodynamic vaporization process (Figure 1) on the T-S plane of methane. GO. . .G7 are the thermodynamic states of the global process. A zoom on the liquid region is reported to show in details the thermodynamic points G0, G1, G2, G3, and G4.

Table I. Process requirements of the liquefied natural gas vaporization facility.

LNG main stream flow rate, G1	186.0 kg/s
BOG evaporation rate, G6, G7	1.86 kg/s
pumps and auxiliary electrical requirement*	15 MW_E
LNG vaporization thermal requirement $Q_{COGEN} = Q_{LNG}$	144 MW_T
specific vaporization thermal requirement	0.77 $MW_T/(kg/s)_{LNG}$
SCV fuel consumption, NG	2.88 kg/s

BOG, boil-off gas; LNG, liquefied natural gas; NG, natural gas; SCV, submerged combustion vaporization.
*Doubled to roughly take into account auxiliary equipments.

summer operation, Kim and Ro [7] proposed the utilization of a LNG chiller that controls the compressor inlet temperature in a GT cycle. Bisio *et al*. [8] gave a detailed II Law thermodynamic analysis of several combined power cycles, realized with different organic fluids. In that paper, a cascade of power cycles from the environment temperature to the LNG temperature, used as a low-temperature thermal source, is envisaged. Kaneko *et al*. [9] proposed to exploit the LNG cold energy by means of 'mirror GTs', a particular kind of combined cycle operated by two gas cycles at different temperatures. Zhang and Lior [10] and Lin *et al*. [11] studied solutions with supercritical CO_2 power cycles that exploit the LNG cryogenic exergy. Shi and Che [12], Miyazaki *et al*. [13], and Qiang *et al*. [14] analyzed solutions with LNG vaporization in the steam condenser of combined cycles. Some recent works propose the exploitation of the LNG stream as a cold source in a cogenerative heat and power plant with a GT and a helium power cycle integrated with an ORV vaporization unit [15]. Integration with Rankine cycles is investigated by Lu and Wang [16] and by Kim *et al*. [17].

Further examples of actual implementations can be found in [18–21]. The vaporization facility of Zeebrugge (Belgium) vaporizes part of the main LNG stream by recovering the energy of the hot exhaust discharged by a GT by means of a water recovery system based on a closed loop and an evaporative cooling tower [18,19].

An example of strong plant integration is given by the EcoElectrica integrated facility installed in the southwest coast of Puerto Rico [20]. The facility includes a 540 MW_E GT combined cycle (GTCC), integrating the LNG vaporization facility of Puerto Rico also with a thermal desalination plant. The whole facility feed Puerto Rico with electric energy (13% of the total demand), NG, and desalted water. This strong plant integration was needed because of environmental impact concerns and guarantees a better primary energy exploitation [20]. In the Higashi-Ohgishima vaporization facility [21], the LNG pressure exergy is exploited by means of direct expansion of the NG stream (from ~100 bar at the exit of the SCV to ~75 bar at the NG network delivery).

The papers cited in the overview so far presented analyze the proposed solutions from several points of view but does not have a common rationale in their performance assessment criteria. Furthermore, some of them are based on strong thermodynamics fundamentals (such as the one by Bisio *et al*. [8]) and are therefore rather difficult to be applied in practical industrial applications. To make the analysis easier to be applied and the results well understandable for the comparison of various possible options, the present paper proposes to adopt a unique parameter (the fuel energy saving ratio (FESR)) based on the primary energy saving concept as the main performance parameter of the system integration and efficiency. Two options of plant integration are presented, and their primary energy saving potential is evaluated with the FESR index. The paper shows that the FESR can be a good means to guide the designer or the manager in the whole energetic choice for the 'best' configuration and to estimate the achievable energy saving.

2. ANALYZED PLANT CONFIGURATIONS AND PERFORMANCE CRITERIA

Two different integrated plant configurations are analyzed. Figure 3 shows the scheme of the first solution analyzed, which is composed by LNG facility coupled to a single GT power cycle. The LNG vaporization thermal requirement is a cogenerative load met by the hot GT exhausts by means of an intermediate glycol loop, suggested to provide a safety heat transfer between air and LNG stream, limiting explosion hazards. The air flow at the compressor inlet is cooled by a bleed of LNG to keep a constant temperature (15 °C). Three different turbine inlet temperatures (T3) have been considered for calculations: 1190 °C (Ansaldo V64.3A [22]), 1288 °C (GE LM6000 [23]), and 1350 °C (Mitsubishi F-series [24]). No auxiliary combustion in the cogenerative heat exchanger that vaporizes the LNG is considered.

Figure 4 shows the scheme of the second solution, composed of the LNG facility coupled to a combined GTCC power plant (CP in this paper). The LNG vaporization thermal requirement is a cogenerative load met by the steam cycle condenser. The very low temperature of the LNG stream does not require back pressure in the steam condenser, thus avoiding the efficiency reductions characteristic of conventional cogenerative power plants. The cold LNG stream guarantees constant inlet temperature at the compressor GC, and it is vaporized in the condenser of the steam bottoming cycle. Heat recovery steam generator (HRSG) has no auxiliary combustion. The GT has the same characteristics of the single GT power cycle configuration, whereas the maximum steam temperature (steam turbine inlet S3H) can be 540, 566, or 600 °C.

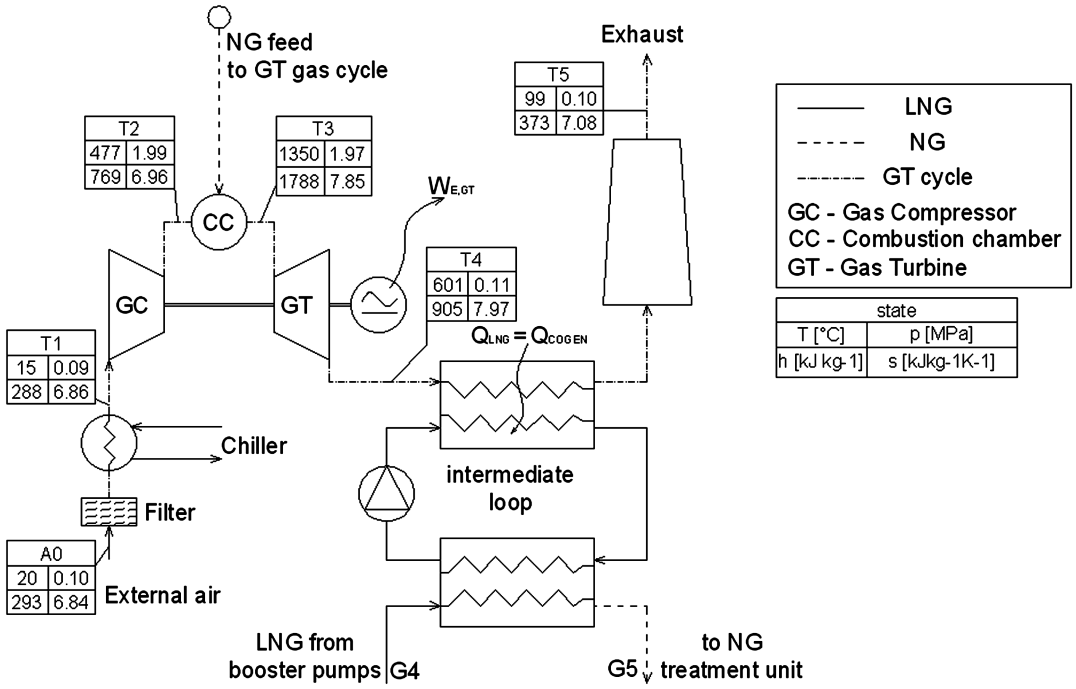

Figure 3. Scheme of the integrated solution composed of a gas turbine (GT) and the SVC-LNG vaporization facility, playing the role of a cogenerative load. The air cycle thermodynamic states are referred to a compression ratio β = 21.8 and Tmax = 1350 °C.

The performance of the integrated plants have been evaluated for all the possible combinations (maximum gas cycle temperature, maximum steam cycle temperature), to give a quantitative assessment of the energy-saving potential in these LNG vaporization facilities.

2.1. Process analysis

The plant performance was evaluated in steady-state regime. The thermodynamic states at the inlet and outlet of each component were computed and hence the energy transfer rates by means of first law energy balances. Actual energy transfer rates are then obtained by means of assumed hydraulic (for pumps), isoentropic (for compressors and turbines), and electromechanical efficiencies.

The thermodynamic states of the fluids are evaluated by means of the software FluidProp [25] with well-established models of fluid properties (TPSI for methane, ideal gas for air, and IAPWS-IF97 for water). The calculation method and the hypothesis are described in detail in the Appendix.

All the main parameters and assumptions used for calculations are reported in Table II. Given the complexity of the CP system and the great number of components involved, all the parameters not specified in the paper has been set to standard default values chosen from an available commercial configuration described in [26].

The main operating parameters that influence the process are the compression ratio β of the GT and the condenser pressure p_{COND} of the steam cycle. Given the technological constraints of the GT group (i.e., the GT inlet temperature), a variation of β induces a modification in the exhaust gas temperatures that influences both the heat rate available at the cogenerative heat exchanger (for the GT plant) or at the HRSG (for the CP plant) and induces a modification in the maximum temperature of the steam cycle. Condenser pressure (p_{COND}) is kept at standard value as the cogenerative load is at low temperature. For this reason, the performance of the cycles is evaluated for different β values, whereas p_{COND} remains unchanged.

2.2. Figures of merit for performance assessment

The figures of merit for a cogenerative plant can be broadly classified in energy conversion indexes (efficiency or 'first law of thermodynamics efficiency') and primary energy saving indexes (usually related to 'second law thermodynamic efficiency').

The energy conversion efficiencies are defined as the ratio between the useful effects (electric power generated) and the energy provided to the system to achieve such effects (combustion power or thermal energy in the steam generator). Equations (1) and (2) are the thermoelectric efficiencies of the GT η_{GT} and of the gas-steam combined cycle η_{CP}.

$$\eta_{GT} = \frac{\dot{W}_{E,GT}}{\dot{Q}_{c.c.}}, \tag{1}$$

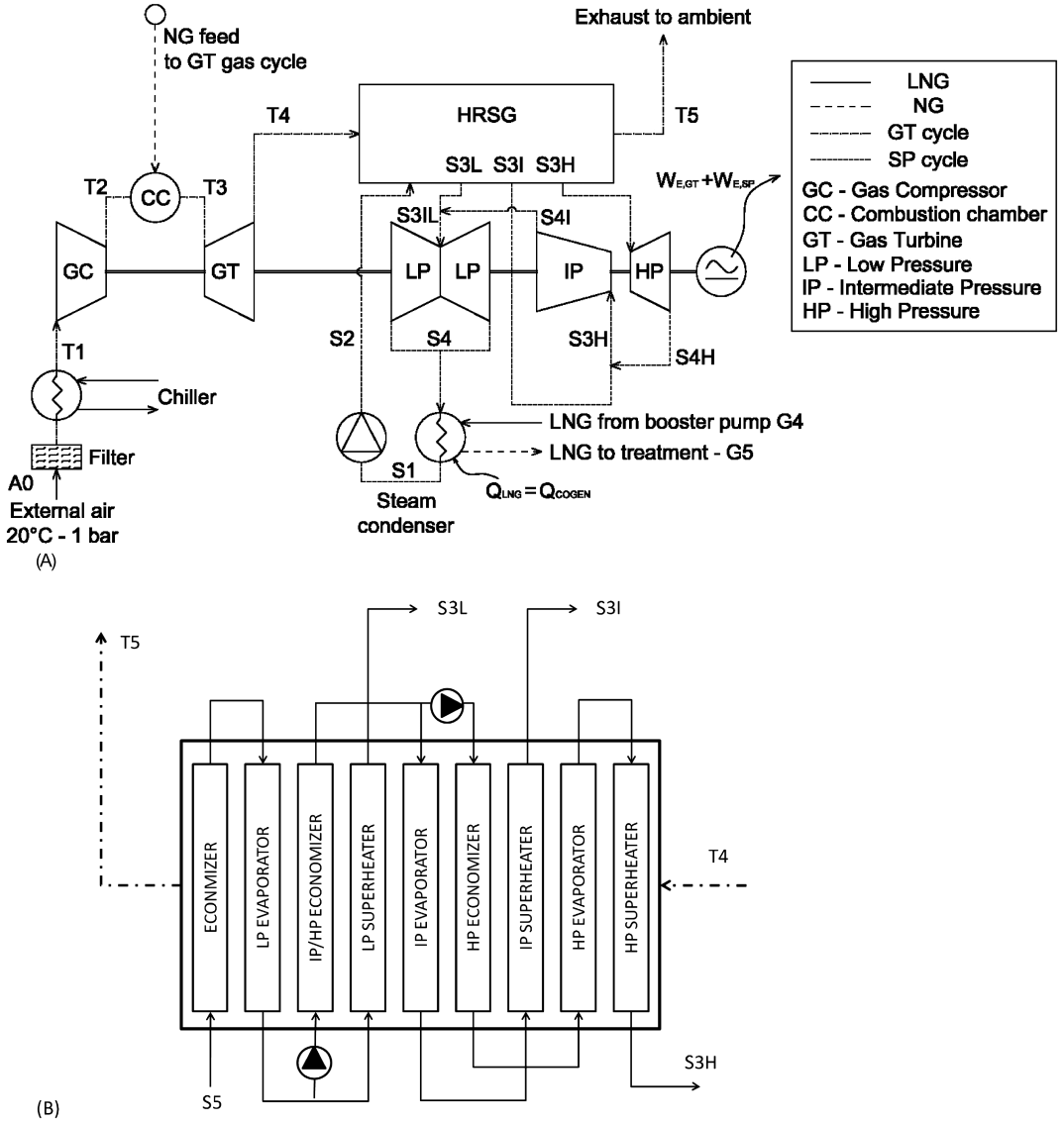

Figure 4. (A) Scheme of the combined plant (CP) integrated solution, composed of a CP and the SCV-LNG vaporization facility applied as a cogenerative load to the steam condenser. (B) Operating scheme of the heat recovery steam generator

$$\eta_{CP} = \frac{\dot{W}_{E,GT} + \dot{W}_{E,SP}}{\dot{Q}_{c.c.}}, \tag{2}$$

$$FESR = 100 - \frac{\left(\frac{\dot{Q}_{c.c.}}{\eta_{c.c.}}\right)}{\left(\frac{\dot{W}_{E,GT}+\dot{W}_{E,SP}}{\eta_{0,GT/CP}} + \frac{\dot{Q}_{COGEN}}{\eta_{0,BOIL}}\right)} \cdot 100 \tag{3}$$

where $\dot{Q}_{c.c.}$ is the heat rate given by the fuel in the combustion chamber of the GT cycle and $\dot{W}_{E,GT}, \dot{W}_{E,SP}$, are the net power output of GT cycle and bottoming steam plant respectively.

Primary energy saving indexes can be employed to perform a consistent comparison between different cogenerative plants and to evaluate the actual primary energy saving that a configuration can perform, for given useful effects and thermal and electrical loads. The FESR reported by El-Nashar [27] is quite well suited to this aim and can be expressed, in percentage, by the following Equation (3).

Considering that in this application, the LNG apparatus is working continuously almost all over the year, the calculations in terms of instantaneous energy rates (electrical power and heat transfer rates) or time-integrated energy data give the same results.

The FESR compares the primary energy (fuel) consumption of the plant to obtain given electrical and thermal useful effects, with the consumption of conventional plants, assumed as reference, able to provide separately the same useful effects. The electric power is

Table II. Main parameters and assumptions adopted for power cycle calculation.

Environment	
Environment temperature	20 °C
Environment pressure	0.10 MPa
LNG vaporization facility	
Size	8 GSm^3/year
Storage temperature T_{tank}	−165 °C
Storage pressure p_{tank}	0.13 MPa
BOG evaporation rate (percentage of main LNG stream)	1.0%
BOG condenser pressure p_{BOG}	0.6 MPa
Sendout temperature $T_{network}$	5 °C
Sendout pressure $p_{network}$	7.5 MPa
Pump hydraulic efficiency	80%
Pump mechanical and electrical efficiency	92%
BOG compressor isoentropic efficiency	85%
BOG compressor mechanical and electrical efficiency	96%
Availability	90%
Gas turbine cycle	
Temperature at turbine inlet	1190–1350 °C
Temperature of released exhaust	99–110 °C
Air intake pressure losses	1.0%
Air temperature at the chiller outlet	15 °C
Compressor isoentropic efficiency	85%
Pressure loss in combustion chamber	2%
Combustion chamber overall efficiency (LHV)	98%
Turbine isoentropic efficiency	90%
Mechanical and electrical efficiency	96%
Heat exchanger air pressure drop	3500 Pa
Steam cycle (parameters from [26])	
Condenser pressure	3.5 kPa
HRSG thermal efficiency	85–90%
HRSG air pressure drop	3500 Pa
Minimum pinch point	11 °C
Low-pressure approach temperature difference	11 °C
Intermediate-pressure approach temperature difference	11 °C
High-pressure approach temperature difference (minimum)	25 °C
Maximum low pressure value	0.46 MPa
Maximum medium pressure value	4.00 MPa
Maximum high-pressure value	14.0 MPa
Low pressure mass flow rate fraction	7.6%
Medium pressure mass flow rate fraction	14.8%
High-pressure mass flow rate fraction	77.6%
Turbine admission temperatures (maximum)	540–600 °C
Steam turbine isoentropic efficiency	87%
Pump mechanical and electrical efficiency	92%
Turbine mechanical and electrical efficiency	96%
Reference efficiencies	
Reference gas turbine efficiency $\eta_{0,GT}$	39.6%*
Reference steam cycle efficiency $\eta_{0,CP}$	60.0%**
Reference boiler/heater efficiency $\eta_{0,BOIL}$ (SCV)	96.0%

*Ansaldo V94.3A
**GE H-Series.
LHV, lower heating value.

supposed to be produced by means of a GT or CP power cycle with the optimal, state-of-the-art, efficiency for the electrical production ($\eta_{0,GT}$ and $\eta_{0,CP}$, respectively) and the thermal power by a conventional boiler with the best available efficiency $\eta_{0,BOIL}$. The numerator in Equation (3) represents the primary energy consumption of the gas burner of the integrated plant. The two terms of the denominator are the primary energy needed

to perform the same electrical production by means of a reference plant optimized for electrical production and the primary energy needed to meet the same heat load with a reference boiler optimized for heat production. The value obtained by Equation (3) gives a clear, concise quantification of the percentage of primary energy saved because of the plant integration. According to the definition given in Equation (3), the FESR index is not intended to compare different plant configurations, but can be used to directly evaluate the benefit of integrated or non integrated plants.

3. RESULTS AND DISCUSSION

3.1. Process analysis of the gas turbine–liquefied natural gas integrated plant

Assuming the complete vaporization of the LNG stream by means of the turbine exhaust, the GT size exceeds the electrical requirements of the plant and allows the electrical power in excess to be delivered to the electric network. A GT limited to electrical self-feeding would guarantee a cogenerative heat rate able to vaporize only the 18% of the LNG stream.

We investigated the influence of the compression ratio β on the GT efficiency and the FESR, for three different turbine inlet temperatures. The results are shown in Figure 5. The maximum shaped trend of efficiency and FESR is caused by the temperature of turbine exhausts heating the LNG. There is an optimum compromise between high electric energy delivery, given by high compression ratios, and high heat energy recovery from exhausts, given by low compression ratios. Obviously, both the FESR and GT cycle efficiency increase with a higher turbine inlet temperature. The lower the inlet temperature, the higher the sensitivity to the β value to achieve best performance. The optimal compression ratio with respect both to FESR and efficiency increases with the inlet temperature. Optimal results are achieved for β in the range of 15–20, with corresponding maximum values for FESR and η_{GT} of 27% and 0.35, respectively.

Table III reports the main process data referred to the operating conditions giving maximum FESR values. The GT is a small-sized GT with efficiency that ranges from low to medium ranges (0.32–0.355). In the configuration with T(T3) = 1350 °C, the efficiency η_{GT} is far from the reference value (0.33 against $\eta_{0,GT} = 0.396$) but guarantees a 27.3% of primary energy saving. It is worth to note that the lower ended solution with $\eta_{GT} = 0.30$ (T(T3) = 1190 °C) also can reduce the primary energy consumption of about the 24.1%. The energy saving is indeed mainly linked to the energy (exergy) recovery in the cogenerative LNG vaporization process, and it is not very much sensitive on GT efficiency. This GT configuration offers an energy saving per year of 2424–2985 GJ/year (which means around 400 k€/year of money savings, without taking into account any possible governmental incentive such as CO_2 emission certificates).

A figure of merit of particular interest can be obtained from these results, assuming the reference of the unit LNG flow rate treated. The GT size range is 81–93.5 MW_E, with a specific electric production of 0.43–0.50 $MW_E/(kg/s)_{LNG}$. The simulation results show that even with low-efficiency and medium-efficiency GT units, an extremely high energy saving is feasible, with specific primary energy savings of 13.0–15.9 (GJ/year)/$(kg/s)_{LNG}$.

3.2. Process analysis of the combined plant–liquefied natural gas integrated plant

The complete vaporization of the whole LNG stream by means of the heat exchanged in the steam condenser is again assumed. Table IV shows the data obtained in nine different configurations, coupling the three GT inlet temperatures with the three maximum steam cycle temperatures. The size of the combined plant for the vaporization of the LNG stream is in the range of 180–200 MW_E, high enough to cover the electric power requirements of the

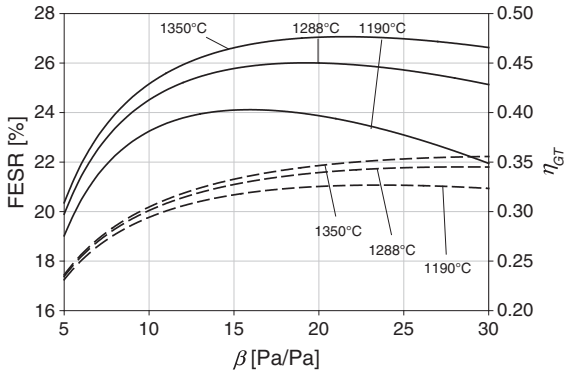

Figure 5. Gas turbine's efficiency (dashed line, scale on the right) and fuel energy saving ratio (FESR; solid line, scale on the left) versus GT cycle compression ratio β. Data are obtained for three different GT inlet temperatures (1190, 1288, and 1350 °C).

Table III. Plant integration with a gas turbine power unit (working conditions giving maximum fuel energy saving ratio) (process calculation).

	T(T3) = 1190 °C	T(T3) = 1288 °C	T(T3) = 1350 °C
Optimal compression ratio β (Pa/Pa)	16.3	19.6	21.8
FESR (%)	24.17	26.21	27.34
η_{GT} (W_E/W_T)	0.30	0.32	0.33
Electric power output (MW_E)	81.1	88.8	93.5
Specific electric power output ($MW_E/(kg/s)_{LNG}$)	0.43	0.48	0.50
Fuel consumption (kg/s)	5.37	5.51	5.60
Specific primary energy saving (GJ/year/$(kg/s)_{LNG}$)	13.0	14.8	16.0

Table IV. Plant integration with a combined plant power unit (optimum fuel energy saving ratio condition) (process calculation).

	T(T3) = 1190 °C		
	T_{MAX}(S3H) = 540 °C	T_{MAX}(S3H) = 566 °C	T_{MAX}(S3H) = 600 °C
Optimal compression ratio β (Pa/Pa)	6.9	6.8	6.7
FESR (%]	16.35	16.44	16.56
η_{CP} (W_E/W_T)	0.48	0.48	0.48
Electric power output (MW_E)	179.5	180.6	182.5
Specific electric power output ($MW_E/(kg/s)_{LNG}$)	0.96	0.97	0.98
Fuel consumption (kg/s)	7.50	7.52	7.56
Primary energy saving (GJ/year)	2076	2097	2127
	T(T3) = 1288 °C		
	T_{MAX}(S3H) = 540 °C	T_{MAX}(S3H) = 566 °C	T_{MAX}(S3H) = 600 °C
Optimal compression ratio β (Pa/Pa)	8.0	8.1	8.0
FESR (%)	17.38	17.47	17.58
η_{CP} (W_E/W_T)	0.49	0.50	0.50
Electric power output (MW_E)	189.0	192.1	194.1
Specific electric power output ($MW_E/(kg/s)_{LNG}$)	1.01	1.03	1.04
Fuel consumption (kg/s)	7.67	7.74	7.79
Primary energy saving (GJ/year)	2286	2323	2355
	T(T3) = 1350 °C		
	T_{MAX}(S3H) = 540 °C	T_{MAX}(S3H) = 566 °C	T_{MAX}(S3H) = 600 °C
Optimal compression ratio β (Pa/Pa)	9.1	9.0	8.9
FESR (%)	17.97	18.05	18.16
η_{CP} (W_E/W_T)	0.50	0.51	0.51
Electric power output (MW_E)	197.5	199.0	201.1
Specific electric power output ($MW_E/(kg/s)_{LNG}$)	1.06	1.07	1.08
Fuel consumption (kg/s)	7.85	7.88	7.93
Primary energy saving (GJ/year)	2435	2460	2492

plant and to deliver electrical power. In each temperature data configuration, an analysis of the performance achievable by varying the compression ratio β has been performed. Maximum shaped trends are obtained (Figure 6) both for FESR and η_{CP} values. The optimal β values are different for each temperature combination and increase with temperature.

The maximum shaped trend is again caused by the balance between the electrical power produced and the heat provided to the cogenerative load. In this configuration, two thermal loads can be identified: the LNG stream (steam condenser) and the HRSG steam generator. The optimal β value is smaller than that in the case of GT-LNG because of the need for more heat to the HRSG and less electrical power production. The efficiency of the GT to achieve optimal global performance of the CP as a whole is decreased to the range of 0.26–0.30.

The maximum FESR and the maximum efficiency η_{CP} conditions for these configurations differ a lot, as shown in Figure 6. For given turbine inlet temperatures, the maximum FESR is obtained with β values much lower than those giving the maximum CP efficiency. This means that FESR and efficiency cannot be optimized at the same time. For example, in the combination 540/1190 (maximum steam temperature/maximum air temperature), the maximum achievable efficiency is $\eta_{CP} = 0.499$ with $\beta = 14.3$,

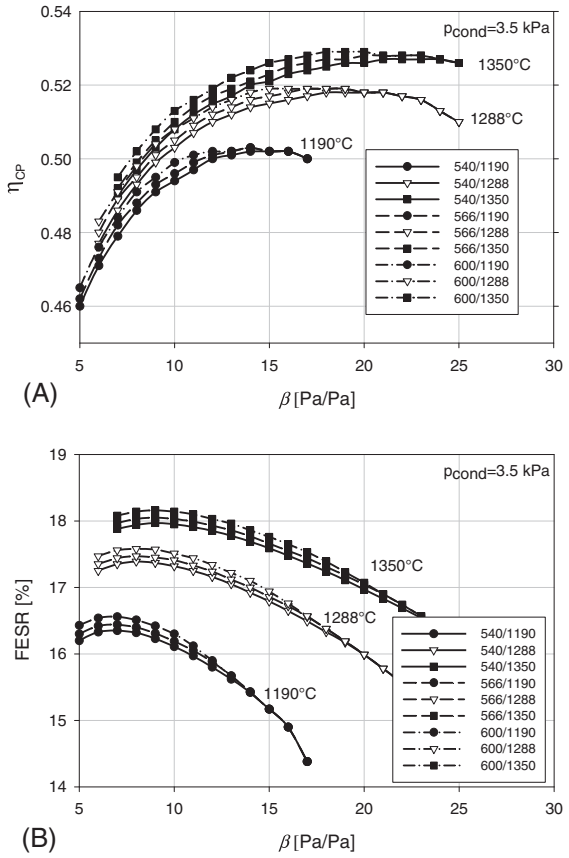

Figure 6. Combined plant efficiency η_{CP} (A) and FESR (B) versus gas turbine compression ratio β. Results for all the temperature combinations (maximum GT inlet air temperature and maximum steam inlet temperature). Different symbols referred to different inlet GT air temperature at point T_3(● = 1190 °C, ▽ = 1288 °C, ■ = 1350 °C) are grouped for the three different inlet steam temperatures at the point S3 (540, 566, and 600 °C).

whereas the maximum achievable FESR is about 16.35% with $\beta = 6.9$. With $\beta = 14.3$, the loss in FESR is 13% (16.35% against 14.30%). Table IV shows that the influence of the maximum steam cycle temperature is weaker than the maximum air temperature. A step of 60 °C (540 °C → 600 °C) in the maximum steam temperature produces a 0.20–0.21% FESR increase, whereas an increase of 62 °C in maximum air temperature (1288 °C → 1350 °C) produces a 0.58–0.59% variation. The same weak influence can be found in the optimal β value that is, on the contrary, strongly influenced by the maximum air temperature. Figure 6 shows clearly this behavior. The performance curves are clearly divided into groups, depending upon the maximum air temperature.

Because the CP has a cogenerative load (the LNG vaporization requirements), another important influence on performance is given by the condensing pressure. However, this is a topic related to all the cogenerative plants, and the influence of p_{COND} is well known (the lower p_{COND}, the higher the performances). The effect of a higher p_{COND} would be a vertical translation toward lower values of the FESR and η_{CP} curves of Figure 6, here not reported for brevity.

In this CP-LNG integrated solution, the cycle efficiencies are low or medium ended (0.50–0.53). Again, despite the relatively low thermoelectric efficiency (with respect to the benchmark efficiency of 0.60 of the Siemens's H-series plant), these solutions offer a primary energy saving of 2090–2508 GJ/year with respect to the separate production of 8 GSm^3/year of vaporized LNG and of 180–200 MW_E produced by a combined power plant with 60% efficiency.

The specific FESR, referred to the unitary LNG flow rate, is calculated and reported for each plant configuration in Figure 7.

It is clearly shown that an integration with a CP is much more oriented to a higher electrical production, whereas a GT integration can only produce about half of the electrical power, given the same cogenerative load. Results shown in Figure 7 must be read carefully. FESR referred to GT is evaluated with a reference efficiency for electrical production of $\eta_{0,GT} = 39.6\%$, whereas FESR referred to CP is evaluated with a $\eta_{0,CP} = 60.0\%$. For this reason, the main information of Figure 7 is the amount of electrical power

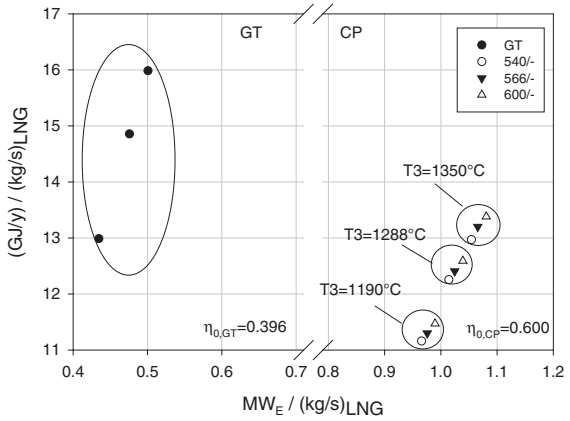

Figure 7. Specific primary energy saving per unit mass flow rate of vaporizing LNG versus specific electric power production. The effect of the temperature in T3 (GT inlet temperature) is predominant. Note the different reference values for the two technologies.

that can be generated for a unitary LNG mass flow rate and the corresponding primary energy saving achievable. A comparison between GT and CP values cannot be performed because of the different reference values. Figure 7 shows again that energy saving capabilities are weakly influenced by maximum steam temperature and much more by maximum gas temperature at the turbine inlet, especially in GT configuration.

4. CONCLUSIONS

Liquefied natural gas vaporization facilities offer an excellent opportunity of primary energy saving by plant integration with power conversion units. This work is focused on the evaluation of the primary energy saving achievable by coupling an SCV LNG vaporization facility with a GT and a CP power plants for electrical production. The performance index FESR, which is commonly used in cogenerative plant performance analysis, compares the fuel (primary energy) requirements of the actual integrated plant and the fuel requirements for separate production of the same useful effects by means of separated, reference plants. This index shows, in an immediate way, the primary energy saving potential of an integrated configuration.

Twelve configurations have been considered, and their steady-state performance has been optimized with respect to FESR by changing the GT compression ratio. Results show that the integration with a single GT can lead to a primary energy saving up to 27%, corresponding to 2985 GJ/year or 15.9 GJ/year per unit mass flow rate of vaporized LNG. The integration with a CP can lead to an energy saving of 18%, corresponding to 2424 GJ/year, that is, 13.0 GJ/year per unit mass flow rate of vaporized LNG. The electrical production capability is 0.43–0.50 MW_E per unit mass flow rate of vaporized LNG for the GT integration and 0.97–1.08 $MW_E/(kg/s)_{LNG}$ for the CP integration.

The investigated solutions could guarantee a meaningful enhancement in environmental sustainability of the LNG vaporization facilities based on SCV technology. Furthermore, all the proposed configurations can be actually realized by arranging standard components based on technologies already available on the market. The primary energy saving evaluation by the FESR methodology, usually applied in the analysis of cogenerative plants, is shown to be reliable and easily understandable, if applied with the proper care. This approach can be used as a good means to guide the designer or manager in the whole energetic choice for the 'best' system plant integration and to give a quantitative assessment of the achievable energy saving.

NOMENCLATURE

Abbreviations

BOG	boil-off gas
CP	combined plant (gas turbine combined plant)
FESR	fuel energy saving ratio (W/W)
GT	gas turbine cycle (unit, plant)
IP	intermediate pressure
HP	high pressure
HRSG	heat recovery steam generator
LNG	liquefied natural gas (liquid state)
LP	low pressure
NG	natural gas (gaseous state)
ORV	open rack vaporization/vaporizer
SCV	submerged combustion vaporization/vaporizer

symbols

h	enthalpy (kJ/kg)
s	entropy (kJ/kg)
$\dot{Q}$	heat rate (W)
$\dot{W}_E$	electrical/mechanical power (W_E)
x	quality

Greek symbols

β compression ratio (Pa/Pa)
η efficiency (W_E/W_T)

subscripts

c.c.	combustion chamber
is	isoentropic
BOIL	relative to boiler/heater
COGEN	of cogeneration
COND	of the condenser
CP	relative to combined plant
E	electrical
GT	relative to gas turbine
HRSG	relative to heat recovery steam generator
T	thermal
0	of a reference plant
SP	steam plant

APPENDIX A

The simulation results are derived from steady-state thermodynamic calculations that are here summarized. The components in the analyzed plants are compressors, turbines, pumps, and heat exchangers. Compressors are described by an isoentropic efficiency $\eta_{is,comp}$ and by a mechanical and electrical efficiency η_{mec}. Given the inlet thermodynamic state, the outlet state and the compressor mechanical power are evaluated as follows.

$$h_{outlet} = h_{inlet} + \frac{h(p_{outlet}, s_{inlet}) - h_{inlet}}{\eta_{is,comp}}$$
$$\dot{W}_{comp} = \dot{m}(h_{inlet} - h_{outlet})/\eta_{mec} \quad \text{(A1)}$$

Turbines are described by an isoentropic efficiency $\eta_{is,turb}$ and by a mechanical and electrical efficiency η_{mec}.

$$h_{outlet} = h_{inlet} - (h_{inlet} - h(p_{outlet}, s_{inlet}))\eta_{is,turb}$$
$$\dot{W}_{turb} = \dot{m}(h_{inlet} - h_{outlet})\eta_{mec} \quad \text{(A2)}$$

Pumps are described by a mechanical and electrical efficiency $\eta_{mec,pump}$. Liquid density ρ is assumed constant.

$$\rho_{outlet} = \rho_{inlet}$$
$$\dot{W}_{pump} = \dot{m}(h_{inlet} - h_{outlet})/\eta_{mec,pump} \quad \text{(A3)}$$

Heat exchangers (air chiller, recovery heat exchangers, and HRSG) have no thermal losses and are characterized by a given pressure drop Δp.

$$\dot{m}_{fluid-1}\Delta h_{fluid-1} = \dot{m}_{fluid-2}\Delta h_{fluid-2}$$
$$p_{outlet} = p_{inlet} - \Delta p \quad \text{(A4)}$$

Gas turbine combustion chamber and SCV are characterized by a thermal efficiency η_{LHV} with respect to the lower heating value and by a pressure drop in the fluid.

$$p_{outlet} = p_{inlet} - \Delta p$$
$$\dot{Q} = \dot{m}(h_{oulet} - h_{inlet})/\eta_{LHV} \quad \text{(A5)}$$

Table A1. Thermodynamic states of air and steam in the optimized combined cycle (compression ratio $\beta = 8.9$, max steam/air temperature 600/1350).

	T (°C)	p (MPa)	Density (kg m^{-3})	h (kJ·kg^{-1})	s (kJ·kg^{-1}·K^{-1})	Quality (x)
			Gas cycle			
A0	20.00	0.101	1.20	293.41	6.84	Superheated
T1	15.00	0.100	1.21	288.39	6.83	Superheated
T2	304.36	0.893	5.37	583.78	6.91	Superheated
T3	1350.00	0.873	1.87	1787.32	8.09	Superheated
T4	764.38	0.105	0.35	1089.68	8.17	Superheated
T5	99.00	0.101	0.95	373.08	7.08	Superheated
			Steam cycle			
S1	26.67	3.5 10^{-3}	996.56	111.82	0.39	0.00
S2	27.42	0.46	996.56	115.37	0.40	Subcooled
S3L	312.59	0.46	1.72	3091.53	7.55	Superheated
S3I	454.04	4.00	12.41	3340.49	6.95	Superheated
S3H	600.00	14.00	37.25	3591.78	6.72	Superheated
S3IL	183.55	0.46	2.25	2822.64	7.03	Superheated
S3HI	415.26	4.00	13.25	3250.40	6.82	Superheated
S4	26.67	3.5 10^{-3}	0.03	2195.31	7.34	0.85
S4I	173.70	0.46	2.30	2801.16	6.98	Superheated
S4H	407.96	4.00	13.42	3233.26	6.80	Superheated

Fluid mixings are assumed adiabatic. All the simplifications and assumptions used in the calculations are here reported (x is quality):

- quality of BOG (state B6), x = 1
- NG delivery conditions constrained
- minimum gas turbine stack temperature T5 = 99 °C
- steam condenser output x = 0
- HRSG vapor quality at the outlet of the economizers, x = 0
- HRSG vapor quality at the outlet of evaporators, x = 1
- HRSG LP steam outlet temperature $T(V3L) = T_{air} - \Delta T_{approach,LP}$
- HRSG IP steam outlet temperature $T(V3I) = T_{air} - \Delta T_{approach,IP}$
- HRSG HP steam outlet temperature $T(V3H) = \min(T_{air} - \Delta T_{approach,HP}, (540/566/600)^{\circ}C)$.

The air temperature along the HRSG is evaluated by means of energy balances for each section $\dot{m}_{air}\Delta h_{air} = \dot{m}_{steam}\Delta h_{steam}$.

In each configuration (for each β and maximum gas/steam temperature couple), the thermodynamic cycle is evaluated with an air to steam mass flow rate ratio $\dot{m}_{air}/\dot{m}_{steam}$ that optimizes the efficiency, with the constrains already given in Table I.

The detailed thermodynamic states of the LNG vaporization facility, the gas turbine plant, and the combined plant in optimal FESR operating conditions are reported on Figures 1 and 2 and in Table A1, respectively.

REFERENCES

1. International Energy Agency. Key world Energy statistics 2008. IEA: Paris, France, 2009.
2. Greipentrog H, Sackarendt P. Vaporization of LNG with closed cycle gas turbine. *ASME paper 76-GT-38*, 1976.
3. Greipentrog H, Weber D. Gasturbinen im geschlossenen Prozeß für neue Anwendungsgebiete. *Kerntechnik* 1978; **20**:537–543.
4. Chiesa P. LNG receiving terminal associated with gas cycle power plants. *ASME paper 97-GT-441*, 1997.
5. Desideri U, Belli C. Assessment of LNG vaporization system with cogeneration. *ASME paper 2000-GT-0165*, 2000.
6. Hanawa K. An Ericsson GT design by LNG cryogenic heat utilization. *ASME paper 2000-GT-166*, 2000.
7. Kim TS, Ro ST. Power augmentation of combined cycle power plants using cold energy of liquefied natural gas. *Energy* 2000; **25**:841–856.
8. Bisio G, Tagliafico LA. On the recovery of LNG physical exergy by means of a simple cycle or a complex system. *Exergy* 2002; **2**:34–50.
9. Kaneko K, Ohtani K, Tsujikawa Y, Fujii S. Utilization of the cryogenic exergy of LNG by a mirror gas-turbine. *Applied Energy* 2004; **79**:355–369. doi:10.1016/j.apenergy.2004.02.007.
10. Zhang N, Lior N. A novel near-zero emission thermal cycle with LNG cryogenic exergy utilization. *Energy* 2006; **31**:1666–1679.
11. Lin W, Huang M, He H, Gu A. A transcritical CO2 Rankine cycle with LNG cold energy utilization and liquefaction of CO_2 in gas turbine exhaust. *Journal of Energy Resources-ASME* 2009; **131**:042201-1–042201-5.
12. Shi X, Che D. Thermodynamic analysis of an LNG fuelled combined cycle power plant with waste heat recovery and utilization system. *International Journal of Energy Research* 2007; **31**:975–998.
13. Miyazaki T, Kang YT, Akisawa A, Kashiwagi T. A combined power cycle using refuse incineration and LNG cold energy. *Energy* 2000; **25**:639–655.
14. Qiang W, Yanzhong L, Xi C. Exergy analysis of liquefied natural gas cold energy recovering cycles. *International Journal of Energy Research* 2005; **29**:65–78.
15. Dispenza C, Dispenza G, La Rocca V, Panno G. Exergy recovery during LNG regasification: Electric energy production – Part one. *Applied Thermal Engineering* 2009; **29**:380–387.
16. Lu T, Wang KS. Analysis and optimization of a cascading power cycle with liquefied natural gas (LNG) cold energy recovery. *Applied Thermal Engineering* 2009; **29**:1478–1484.
17. Kim CW, Chang SD, Ro TS. Analysis of the power cycle utilizing the cold energy of LNG. *International Journal of Energy Research* 1995; **19**(9):741–749.
18. Yang CC and Huang Z. Lower emission LNG vaporization. *LNG Journal* 2004; **6**: 24–26.
19. Pairon JL, Gabriel JJ. Cogeneration as a solution to reduce the energy consumption of the submerged vaporizers. *Proceedings of the "LNG 11 Congress"*, Birmingam, United Kingdom, 1995.
20. http://www.ecoelectrica.com/ourfacilities/index.html (20 April 2011).
21. Tokyo Electric Power Company, *Annual report 2006*, 2006.
22. Ansaldo energia, *Gas Turbine*, www.ansaldoenergia.com/PDF/Gas_Turbines.pdf. (20 April 2011).
23. Badeer GH (GE Power systems). GE Aeroderivative gas tubines – design and operating features, www.gepower.com/prod_serv/products/tech_docs/en/downloads/ger3695e.pdf. (20 April 2011).
24. Mitsubishi heavy industries LTD, http://www.mhi.co.jp/en/products/expand/f_series_gas_turbine_development_01.html. (20 april 2011).

25. FluidProp Software for the calculation of thermophysical properties of fluids, Delft University of technology, Nederlands, http://fluidprop.tudelft.nl. (20 April 2011).
26. Chase DL, Kehoe PT, (GE Power systems), GE Combined-cycle product line and performance, www.gepower.com/prod_serv/products/tech_docs/en/downloads/ger3574g.pdf. (20 April 2011).
27. El-Nashar AM. Cogeneration for power and desalination – state of art review. *Desalination* 2001; **134**:7–28.